

# Si-incorporated alumina phases formed out of diphasic mullite gels

A. K. Chakraborty

Received: 12 July 2006 / Accepted: 4 June 2008 / Published online: 24 June 2008  
© Springer Science+Business Media, LLC 2008

**Abstract** The diphasic mullite gel forms *o*-mullite on heating via intermediate spinel phase. Characterization of the latter phase with various physico-chemical techniques is concisely reviewed. It is noticeable that XRD intensity of both the amorphous scattering band and the diffraction peak of Al–Si spinel phase changes during each step of transformation processes of diphasic gel. Accordingly, the integrated area of the intensity peak of amorphous band and that of Al–Si spinel phase generated during heating diphasic gels were measured by XRD technique with the help of X’Pert Graphics and Profit softwares. The amount of free SiO<sub>2</sub> (A) content present at various stages of heating diphasic gels was estimated by classical alkali leaching study standardized earlier. The results show that diphasic gel which forms an aluminosilicate (A) phase initially by dehydration and dehydroxylation, subsequently crystallizes to Al–Si spinel phase. In consequence, the ratio of XRD peak of spinal phase to that of amorphous band increases in the temperature range of 600–1000 °C. This study confirms the earlier view of incorporation of silica into the alumina structure with formation of Al–Si spinal phase. Complementary alkali leaching study indicates the existence of non-crystalline silica-rich aluminous phase other than free non-crystalline silica during heating diphasic gel at ~1000 °C.

## Introduction

Extensive studies have been made to the processing and characterization of sol–gel-derived mullite. It is thought that mixing scale of the two components controls the reaction course to mullite [1]. This is varied by the processing parameters chosen for sol–gel precursors which in turn guide the path of phase transformation and temperature of mullite formation. It is well known that each transformation path consists of few steps.

At the first step, monophasic gel dehydrates and removes adhered organics. On the other hand, diphasic gel at the first step decomposes into amorphous alumina and amorphous silica, and partially crystallizes to  $\gamma$ -Al<sub>2</sub>O<sub>3</sub>

In the second step, Al<sub>2</sub>O<sub>3</sub>–SiO<sub>2</sub> gel named either as monophasic or slow hydrolysis (SH) or Polymeric or Type I gel directly transformed to *t*-mullite at the occurrence of 980 °C exotherms [2]. In some kind of monophasic gel, a third step is noted. This monophasic gel first forms either a weakly crystalline spinel phase as a single crystalline phase or a mixture of it and *t*-mullite at 980 °C exotherm. Later, this spinel phase transforms to *o*-mullite at the 2nd exotherm ~1250 °C at the third stage. At the second stage, two discrete alumina and silica phases of decomposed diphasic gel form an intermediate spinel phase like the one that crystallizes in the case of monophasic gel but without any exhibition of 980 °C exotherm.

At the third stage, this spinel phase transforms to *o*-mullite with exhibition of an exotherm at ~1300 °C. Regarding the character of this intermediate spinel phase whether it is  $\gamma$ -Al<sub>2</sub>O<sub>3</sub> spinel or silicon-substituted alumina spinel (Al–Si spinel), some indirect experimentations have been conducted [3–13]. By QXRD estimation of mullite, the present author [13] further showed that the course of its formation from diphasic gels and mixed oxides are dissimilar in nature.

---

A. K. Chakraborty (✉)  
Refractories, Central Glass and Ceramic Research Institute,  
Kolkata 700 032, India  
e-mail: akshoyc@hotmail.com

Suddenness of mullitization indicated that intermediate spinel phase in two reacting systems are totally different. Earlier by QXRD analysis of spinel phase, Chakraborty and Das [11] showed that measured X-ray intensities at  $46^\circ$  and  $66^\circ$   $2\theta$   $\text{CuK}_\alpha$  radiation of spinel phase formed out of diphasic gels were much greater than that of the theoretical intensities expected for  $\gamma\text{-Al}_2\text{O}_3$  phase formation. The result of increase in intensities of spinel phase on heat treatment was explained to be due to incorporation of silicon in the  $\gamma\text{-Al}_2\text{O}_3$  spinel phase. And lastly by comparative phase evolution process by the present author [13] it was also shown that some diphasic gels (composition of  $\text{Al}_2\text{O}_3$  up to 72 wt.%) do not crystallize in to a combined mixture of  $\theta\text{-Al}_2\text{O}_3$  and  $\alpha\text{-Al}_2\text{O}_3$  polymorphs at the intermediate stage prior to mullite formation during heating process. These results convince more to the formation of Al–Si spinel phase instead of  $\gamma\text{-Al}_2\text{O}_3$ . Besides Al–Si spinel formation, it also indicates that the so-called  $\theta\text{-Al}_2\text{O}_3$  which forms as in the intermediate stage also contain  $\text{SiO}_2$  and it decomposes to mullite and  $\alpha\text{-Al}_2\text{O}_3$  on further heating instead of crystallization of both forms of  $\theta\text{-Al}_2\text{O}_3$  and  $\alpha\text{-Al}_2\text{O}_3$ .

With these experimental results as put forward by various authors, it is beyond doubt to admit that the controversial cubic phase is Al–Si spinel. The changes in XRD intensity of it was noted by Okada and Otsuka [2], and subsequently by Chakraborty and Das [11]. However, literature regarding the changes in intensity of X-ray amorphous band due to either silica (A) or other amorphous phase during heat treatment of  $\text{Al}_2\text{O}_3\text{-SiO}_2$  gels up to mullitization is very scarce. Recently, Ivankovic et al. [14] calculated the integrated area of spinel peak at  $46^\circ$   $2\theta$  and same for amorphous band (assuming silica peak) at  $22^\circ$   $2\theta$  for gel samples heat treated to 800 and 1000  $^\circ\text{C}$ , respectively to find the way of crystallization process of Al–Si spinel formation. In this method they observed that hump of the amorphous band was decreased; at the same time the intensity of spinel phase was increased and no mullite was formed. Observing the decrease in the intensity of the amorphous band (the amount of amorphous silica) at  $22^\circ$   $2\theta$ , they concluded that sample marked B (a combination of type II and type III gel showed pseudo boehmite at the gel state) gel formed Al–Si spinel by incorporation of silica into  $\gamma\text{-Al}_2\text{O}_3$  as shown by Schneider et al. [15] for their Type II gel synthesized out of TEOS and  $\text{AlOBU}$  at strongly basic condition. However, during the measurement

of XRD intensities of amorphous band and same for Al–Si spinel phase, they selected background manually during calculation of integrated intensities of both amorphous band and Al–Si spinel phase.

In the present investigation, we intend to study how the intensity of X-ray amorphous band changes during heat treatment of diphasic gel form  $\sim 400^\circ\text{C}$  onwards instead of measuring XRD intensities only at some predetermined temperatures up to 1000  $^\circ\text{C}$  as per Ivankovic et al. [14]. Intensities of both the amorphous scattering band and the diffraction peak of Al–Si spinel phase are very small. In the first approach, the integrated areas for amorphous band and spinel phases formed out of diphasic gels of varying compositions heat treated at different temperatures are measured using X'Pert graphic software with the use of internal standard, e.g.,  $\text{CaF}_2$  as calibrant to prove that the method works relatively well.

In the second approach, diphasic gels are heat treated to different temperatures and leached for free amorphous silica content by alkali leaching study. The results of two experimentations substantiate the earlier view of incorporation of Si in phase.

## Experimental procedure

### Synthesis of diphasic gels

Three diphasic gels differing in  $\text{Al}_2\text{O}_3$  weight ratio were synthesized by using aluminum nitrate nonahydrate (ANN, AR quality) and tetra ethyl orthosilicate (TEOS, BDH make) as shown in Table 1. Weighed quantities of two components of each gel were taken in a pyrex beaker. To it, required quantities of double-distilled water and ethyl alcohol were added and warmed to 60  $^\circ\text{C}$  followed by stirring until the ANN crystal dissolves and alcoholic layer disappeared from the solution and finally cooled. The solution was adjusted to pH 9 by adding ammonia solution in the stirring condition. The gelatinous slurry was dried at 120  $^\circ\text{C}$  and stored.

### Heat treatment and XRD analysis

All dried gel samples were heat treated to different temperature ranges from 600 to 1400  $^\circ\text{C}$  for 2 h soaking in

**Table 1** Synthesis of three different compositions of diphasic gels

Mark of diphasic gel	Wt. of finished gel (dry basis) (g)	$\text{Al}_2\text{O}_3\text{:SiO}_2$ ratio (wt.%)	Amount of TEOS (mL)	Amount of ANN (g)	Amount of water (mL)	Amount of alcohol (mL)
DG40	18.4	40:60	80	100	1000	200
DG66	16.2	66:34	40	150	1500	100
DG72	20.0	72:28	40	200	2000	100

**Fig. 1** (a) Shows the phase evolution of representative diphasic gel marked DG40; S: Spinel, M: Mullite. (b) Shows the phase evolution of representative diphasic gel marked DG66; A: Aluminosilicate phase

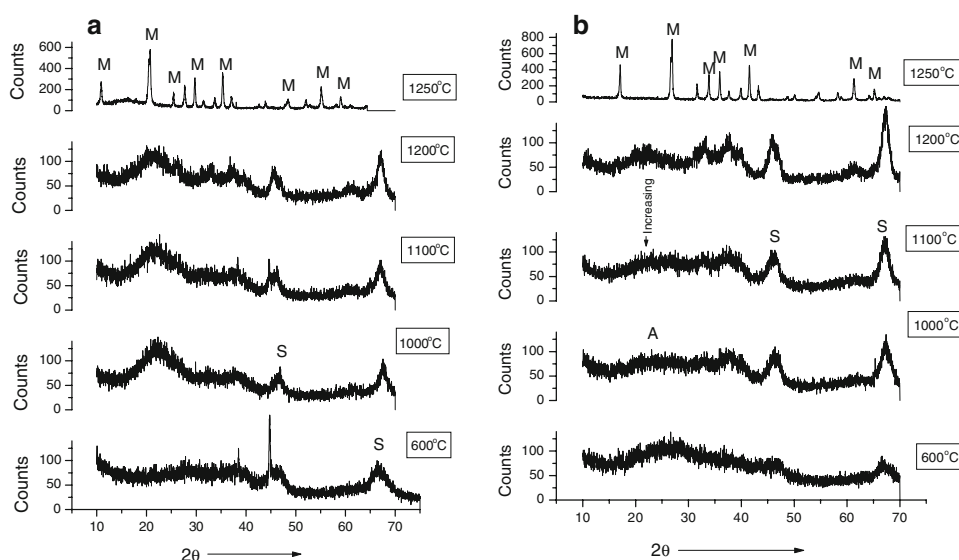
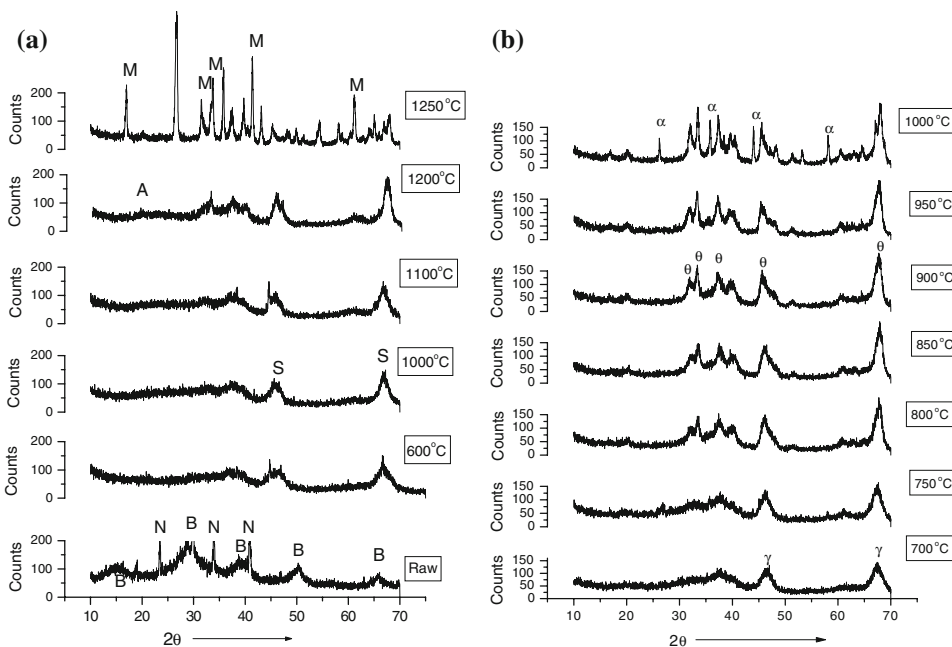


**Fig. 2** (a) Shows the XRD pattern of raw DG72 and heated to 600, 1000, 1100, 1200, and 1250 °C after smoothening; B: Boehmite, N: free NH<sub>4</sub>NO<sub>3</sub>. (b) Shows the XRD pattern of pure alumina gel after heating at 700, 750, 800, 900, 950, and 1000 °C showing  $\gamma$ -Al<sub>2</sub>O<sub>3</sub> at the beginning and thence  $\theta$ -Al<sub>2</sub>O<sub>3</sub> and lastly a mixture of  $\theta$ -Al<sub>2</sub>O<sub>3</sub> and  $\alpha$ -Al<sub>2</sub>O<sub>3</sub>



each case in an electric furnace, cooled and stored. For phase identification, the ground samples were analyzed by Philips<sup>1</sup> XRD generator model PW1730 attached with graphite monochromator and fitted with PW 1710 counting electronics with a computer. The tube was run at 40 kV/20 mA CuK<sub>α</sub> radiation. The diffractogram patterns were taken for different heat-treated gel conditions and are shown in Figs. 1–3. Phases formed during heat treatment of those diphasic gels at different temperatures were identified using ICDD files and are shown in Table 2.

<sup>1</sup> Spectrics Technologies, PW 1730 with PW 1710 electronics.

Measurement of XRD intensities of amorphous band and spinel phases

For measuring amorphous band intensity, heated gel samples were mixed and ground with 10 wt.% CaF<sub>2</sub> for ½ h with alcohol and finally dried. For XRD analysis, the tube was run at 40 kV/20 mA radiation, scan rate-step scan technique at the size of 0.04° 2θ with 0.5 s as time per step using CaF<sub>2</sub> as an internal standard for calibration intensities of amorphous phase and spinel phase, respectively. An average of three estimated intensity data of those phases at each temperature is plotted in Figs. 4 and 5.

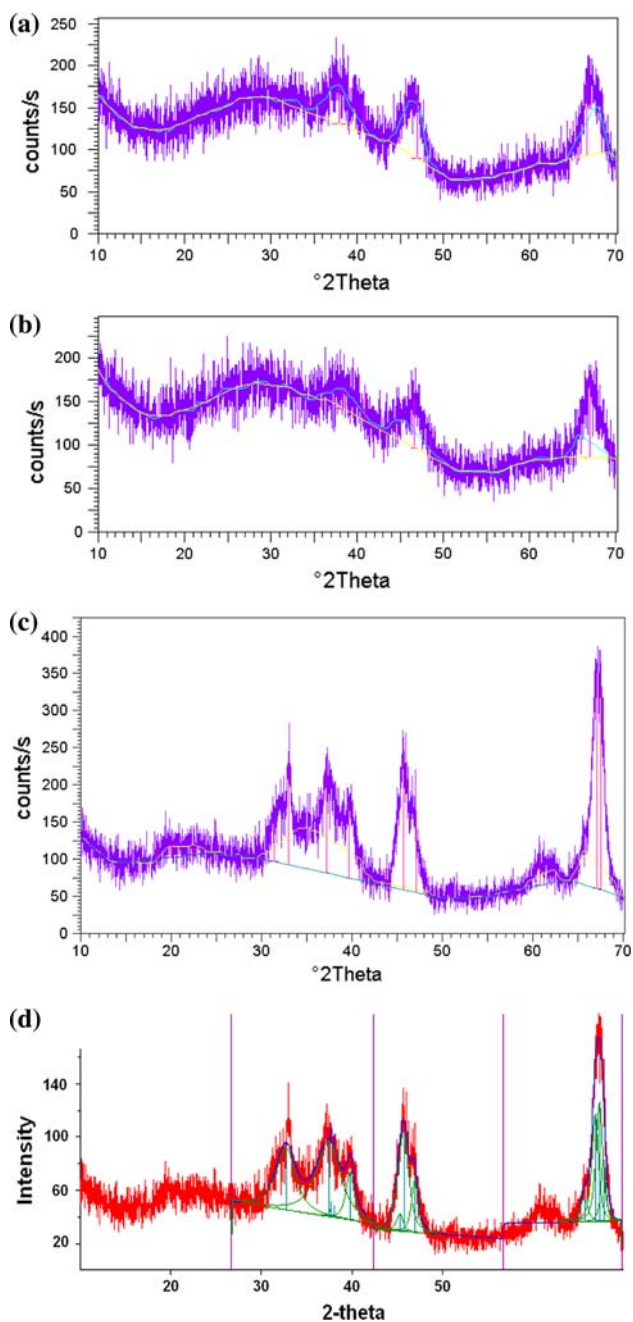


**Fig. 3** (a) DG72 gel heated to 700 °C shows a single peak at 46°  $2\theta$  and 66°  $2\theta$ . (b) DG72 gel heated to 900 °C shows a single peak at 46°  $2\theta$  and 66°  $2\theta$ . (c) The above gel heated to 1200 °C shows two peaks at 46°  $2\theta$  and 66°  $2\theta$ . (d) The profit data of above heat-treated gel shows peaks around 46°  $2\theta$  and at 66°  $2\theta$

*First approach: measurement of XRD intensities of amorphous band and Al–Si spinel phase*

XRD intensities of 0.139 nm peak at 67°  $2\theta$  of Al–Si spinel and 0.164 nm peak at 55.8°  $2\theta$  of  $\text{CaF}_2$  were scanned for calculation of area of Al–Si spinel to  $\text{CaF}_2$ .

Secondly, XRD intensities of 0.40 nm peak at 22°  $2\theta$  of amorphous band and 0.164 nm peak of  $\text{CaF}_2$  were scanned for calculation of area of amorphous band to  $\text{CaF}_2$ . Area of the amorphous hump and integrated area under the peak of spinel phase formed during heating diphasic gels were finally calculated with the help of X’Pert graphic software supplied by the Philips and are shown in Table 3. It shows a comprehensive picture of the changes in intensities of the amorphous band and also the spinel phase formed on heat treatment of three different diphasic gels at successive increase of temperatures. These data are subsequently plotted and are shown in Figs. 4 and 5, respectively. The nature of the curve as shown in Fig. 5 agrees with that shown earlier by Okada and Otsuka [2] and Chakraborty and Das [11].

*Alkali extraction study*

*Second approach: measurement of free silica (A) by alkali leaching study*

Heat-treated gels were leached by NaOH solution as mentioned previously [3]. 0.5 g of ground sample was treated with 10 mL of 5 wt.% alkali solution in boiling water bath condition for 40 min duration for each case. After alkali treatment, it was centrifuged and washed. The centrifugate and washings were analyzed for  $\text{SiO}_2$  and  $\text{Al}_2\text{O}_3$  by gravimetric procedure. Percentage of leached  $\text{SiO}_2$  and  $\text{Al}_2\text{O}_3$  of different diphasic gels vs. heat treatment temperature are plotted in Fig. 6. These results agree with the earlier data in case of thermal transformation of kaolinite studied by alkali leaching [3].

**Results**

*Identification of intermediate alumina bearing phases*

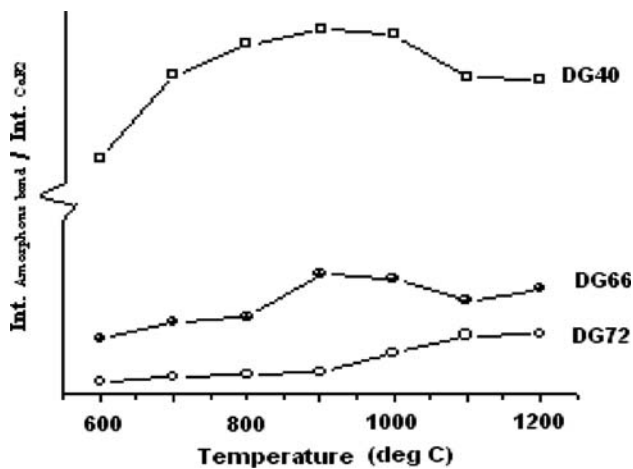
Crystallization pathways of diphasic gels of different compositions and pure alumina gel have been studied by X-ray analysis. Figures 1a, b, and 2a show the phase evolution of diphasic gels marked DG40, DG66, and DG72, respectively. Boehmite phase present in raw diphasic gel first decomposes during heating at ~400 °C. It, thereafter, develops spinel phase gradually on further heating from 500 to 1200 °C. At ~1250 °C, it structurally changes to *o*-mullite. In comparison to the phase evolutions of DG40, DG56, and DG72, the sequential changes of phases that occurred during the heat treatment of pure aluminum hydroxide gel are shown in Fig. 2b. Apparently, phase development processes of DG40, DG66, and DG72 show variations from that of pure alumina gel. Direct comparison of the characteristic XRD peaks of spinel

**Table 2** Phase identification of diphasic mullite gel during heating

$\gamma$ -Alumina			$\delta$ -Alumina			$\theta$ -Alumina		Mullite gel heated to			
$d$ (Å)	$I$	$hkl$	$d$ (Å)	$I$	$hkl$	$d$ (Å)	$I$	1000 °C		1200 °C	
			7.97	8	100						
			6.58	10	101						
			5.85	1	002						
						5.46	10				
			5.07	20	111						
			4.71	3	102						
			4.95	20	112						
4.55	10	111									
						4.53	30				
			3.75	2	201						
			3.56	7	210						
						3.53	3				
			3.40	10	211						
			3.28	15	202						
			3.21	10	113						
			3.03	10	212						
						2.84	80			2.84	18
			2.783	30	203						
2.782	15	220									
			2.737	30	104;221						
						2.72	100	2.73	19	2.71	44
			2.593	70	114						
						2.564	20				
			2.457	70	311						
						2.439	90			2.41	44
2.398	90	440						2.39	42		
2.387	35	311									
						2.314	60				
			2.311	40	312						
2.283	20	222									
			2.277	30	223	2.254	50	2.27	31	2.26	33
			2.156	25	115						
						2.018	60				
1.977	100	400	1.989	70	400			1.98	64	1.98	57
			1.950	65	006	1.955	15	1.94	49		
						1.907	35			1.92	34
			1.833	2	412						
						1.801	15				
			1.796	7	225					1.79	2
						1.773	7				
			1.759	3	421						
						1.734	5				
			1.730	1	413						
			1.701	4	422						
						1.621	7				
			1.602	15	226;117						
			1.572	1	306						

**Table 2** continued

$\gamma$ -Alumina			$\delta$ -Alumina			$\theta$ -Alumina		Mullite gel heated to			
$d$ (Å)	$I$	$hkl$	$d$ (Å)	$I$	$hkl$	$d$ (Å)	$I$	1000 °C		1200 °C	
						1.568	8				
			1.543	10	316	1.542	30				
1.521	10	511				1.510	8	1.51	15	1.52	10
			1.507	20	512	1.486	20				
			1.462	8	335;326						
			1.435	2	522						
			1.407	60	440			1.40	100		
1.398	90	440	1.392	100	406	1.404	40				
						1.388	90			1.39	100
						1.295	10				
						1.285	10				
						1.259	6				
			1.248	10	525						
			1.235	10	209						

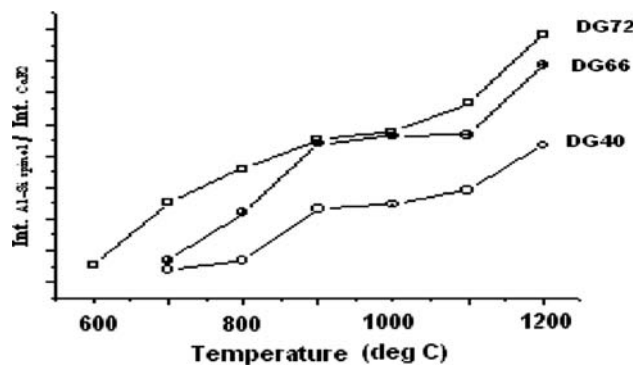
**Fig. 4** X-ray amorphous band of diphasic gel heat treated to different temperatures

phase formed out of DG72 at  $\sim 1000$  °C to that of pure  $\gamma$ - $\text{Al}_2\text{O}_3$  and  $\delta$ - $\text{Al}_2\text{O}_3$  are shown in Table 2.

#### Characterization of amorphous band

##### By XRD technique

Nature of changes in intensities of X-ray amorphous bands developed during heat treatment of diphasic gels of three compositions is shown in Fig. 4. Each plot shows three distinct steps.

**Fig. 5** Ratio of  $I_{\text{Al-Sisipinel}}/I_{\text{CaF}_2}$  of diphasic gel vs. heat treatment temperature

In the first step of transformation process, the amorphous band increases in the temperature range (600–900 °C). Depending upon the composition of each diphasic gels, the plots show that it increases slowly in case of DG72 and it raises very fast in case of DG40, but in case of DG66 the increase is moderate. In the second step, the band intensity decreases sharply in the temperature range of 900–1100 °C for all three such diphasic gels marked DG40, DG56, and DG72.

In the third step, the amorphous band still persists in the temperature range of 1100–1200 °C. Figure 4 shows that the intensity of amorphous band remains constant with heat treatment in the above temperature range in the case of DG40. However, it first decreases and then increases in the



**Table 3** Changes in XRD intensities of amorphous band and Al–Si spinel phase derived out of heat treatment of three kinds of diphasic gels in the presence of CaF<sub>2</sub> as calibrant

Gel mark	Heat treat temp. (°C)	XRD counts 22° 2θ band	XRD counts 55.8° 2θ CaF <sub>2</sub>	Ratio of I <sub>band</sub> /I <sub>CaF<sub>2</sub></sub>	XRD counts 66° 2θ spinel	Ratio of I <sub>spinel</sub> /I <sub>CaF<sub>2</sub></sub>	Ratio of I <sub>spinel</sub> /I <sub>band</sub>
DG40	600	627.5	60	10.46	–	–	–
	700	952	68	14.0	92	1.36	0.096
	800	950.5	62	15.33	105	1.7	0.110
	900	909	57	15.95	190	3.33	0.209
	1000	882	56	15.75	193.7	3.46	0.219
	1100	977	70	13.96	273	3.91	0.279
	1200	998	72	13.86	383	5.33	0.383
DG66	600	159.6	56	2.85	57	1.01	0.357
	700	223.6	63	3.55	105	1.68	0.469
	800	230.6	61	3.78	195	3.2	0.845
	900	381.5	68	5.61	365	5.38	0.956
	1000	360.5	67	5.38	377	5.63	1.047
	1100	276.5	62	4.46	351	5.66	1.269
	1200	283	57	4.98	449	7.88	1.586
DG72	600	54.5	54	1.01	82	1.53	1.50
	700	71.3	57	1.25	199	3.5	2.791
	800	80	60	1.33	276	4.6	3.45
	900	88.6	62	1.43	340	5.51	3.837
	1000	131.6	59	2.23	339	5.75	2.575
	1100	172.84	58	2.98	387	6.68	2.339
	1200	170.8	56	3.05	495.6	8.85	2.901

case of DG66. Contrarily, it gradually increases in the case of DG72 from 1100 to 1200 °C.

*By alkali leaching technique*

The alkali leaching data of three diphasic gels heat treated to different temperatures are shown in Fig. 6. The plots show three important observations.

- i. In the temperature range of 600–900 °C, silica component of diphasic gels marked DG72 dissolves in hot alkali solution to the extent of only ~2.5% out of 28% present originally. This indicates that silica component which remained as separate and individual component of two-phase system after dehydration and decomposition of diphasic gels at ~400 °C becomes insoluble in hot alkali solution when it is heated to 600 °C.
- ii. At ~1000 °C, Fig. 6 (lower curve) shows that a portion of silica liberates during heating those diphasic gels. Thereafter, it becomes more or less constant even with further heating. The approximate quantity of silica (A) dissolved at 1000 °C in alkali solution in three

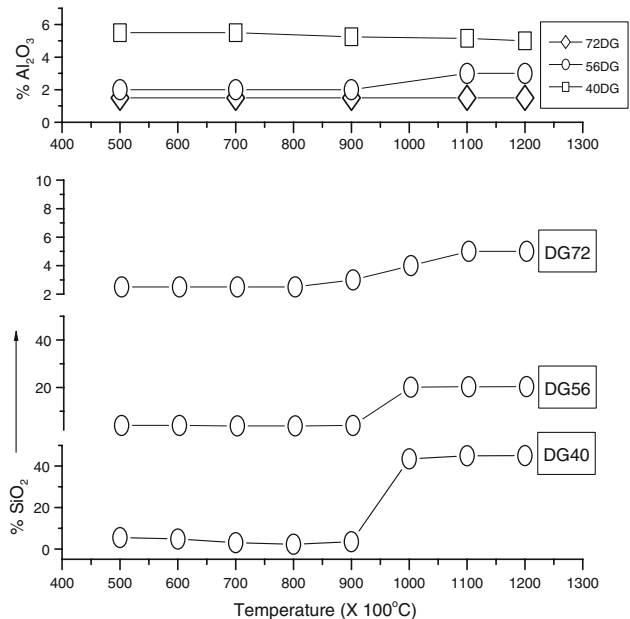


**Fig. 6** Alkali leaching of diphasic gel heat treated to different temperatures





At the first stage, i.e., in the temperature range between 600 and 900 °C, spinel formation occurs slowly in all three cases of diphasic gels (Fig. 5). Some of the pertinent points regarding the nature of this intermediate spinel phases formed as shown in the Table 2 are discussed below.

- i. XRD intensities of some peaks of spinel phase formed out of heating DG40, DG66, and DG72 are largely different from pure  $\gamma$ - and  $\delta$ - $\text{Al}_2\text{O}_3$ .
- ii. Some of the peaks of it are missing. All characteristic peaks of it do not correspond to either  $\gamma$ - or  $\delta$ - $\text{Al}_2\text{O}_3$  (JCPDS file Nos., 46-1215, 04-0877, 47-1770, 46-1131, etc.) so far its intensities and peak positions are concerned. Thus, intermediate spinel phase derived out of DG72 could not conclusively be identified as  $\gamma$ - $\text{Al}_2\text{O}_3$  or as  $\delta$ - $\text{Al}_2\text{O}_3$ . Contrarily, the XRD data of heated DG72 indicated below incline more in favor of the development of Al–Si spinel phase.

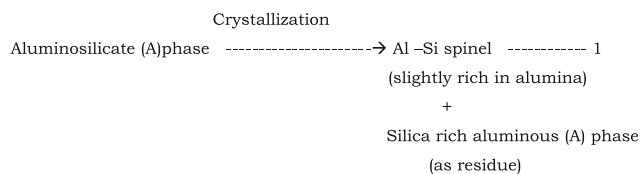
The pattern does not show crystallization of either cristobalite or corundum even on heating gel at 1200 °C, i.e., independent crystallization sequence of the alumina component is modified in the presence of silica. Alumina also suppresses the formation of cristobalite. The reason to the question of suppression might be due to substantial incorporation of silica in  $\gamma$ - $\text{Al}_2\text{O}_3$  structure and it may be the reason of non-crystallization of either corundum or cristobalite when  $\text{Al}_2\text{O}_3$ – $\text{SiO}_2$  mullite gel was heat treated to higher temperature.

- iii. The XRD intensity 0.140-nm peak of spinel phase increases gradually with increase of heat treatment temperature in the range of 1000–1200 °C. Thus, it exists at as high as 1200 °C. The stability at high temperature indicates that  $\text{Si}^{+4}$  substitutes tetra covalent aluminum of  $\gamma$ - $\text{Al}_2\text{O}_3$  phase during heating process of  $\text{Al}_2\text{O}_3$ – $\text{SiO}_2$  diphasic gel and forms silica-incorporated  $\gamma$ - $\text{Al}_2\text{O}_3$  phase (called as Al–Si spinel). This process may result in increase of strain in spinel lattice which may be the reason for the loss of some characteristic XRD peaks of spinel phase and poisoning of further phase transformation of it to corundum.
- iv. The shape of XRD intensity peaks of spinel phase at  $46^\circ 2\theta$  and  $66^\circ 2\theta$  derived out of diphasic gels heated to 700–900 °C appears uniform (Fig. 3a, b). At the higher heat-treatment temperature at  $\sim 1200$  °C, asymmetry is observed and each of those peaks could be resolved on deconvolution (Fig. 3c). Two peaks are observed at  $46^\circ 2\theta$  region during peak search operation using graphics software, first one at  $45.71^\circ$ , second one at  $47.08^\circ$ , respectively which resembles near to  $\theta$ - $\text{Al}_2\text{O}_3$ . Similar observation is noted during profile fitting of the said XRD pattern (Fig. 3d) using X'Pert Profit software. These observations apparently indicate

that a fraction of silica-incorporated  $\gamma$ - $\text{Al}_2\text{O}_3$  phase likely transforms to silica-incorporated  $\theta$ - $\text{Al}_2\text{O}_3$  phase during gradual heat treatment from 1000 to 1200 °C. The existence of this phase far above 1000 °C was noted earlier by Iller [17] and Yoldas [18, 19] in case of heating  $\text{Al}_2\text{O}_3$ – $\text{SiO}_2$  gels and explained the stabilizing effect as the role of some % of silica which was introduced into the  $\theta$ -structure and delayed further crystallization to  $\alpha$ - $\text{Al}_2\text{O}_3$ . Iller [17], Wakao and Hibino [20], and Saito et al. [21] also showed the existence of  $\theta$ - $\text{Al}_2\text{O}_3$  in gels made out of colloidal particles increased to the extent of 100–200 °C more than pure gel components. In a parallel reaction, some amount of silica may get incorporated into  $\gamma$ - $\text{Al}_2\text{O}_3$  phase and develops Si-incorporated  $\theta$ - $\text{Al}_2\text{O}_3$  phase.

Chakraborty [22, 23] showed the persistence of  $\gamma$ - $\text{Al}_2\text{O}_3$  much above 1100 °C in both impregnated and mixed  $\text{Al}_2\text{O}_3$ – $\text{SiO}_2$  gels. This result is in contrast to its normal transition of boehmite gel at  $\sim 1050$  °C to  $\theta$ - $\text{Al}_2\text{O}_3$ . It was presumed that during heating processes of both gels, Si penetrates into the newly formed  $\gamma$ - $\text{Al}_2\text{O}_3$  and develops Si-substituted  $\theta$ - $\text{Al}_2\text{O}_3$ . This substitution probably causes enhancement of its transformation temperature from 1100 to 1200 °C. By comparative phase evolution process, the present author [13, 22] also showed that some diphasic gels (composition of  $\text{Al}_2\text{O}_3$  up to 72 wt.%) did not crystallize in to a combined mixture of  $\theta$ - $\text{Al}_2\text{O}_3$  and  $\alpha$ - $\text{Al}_2\text{O}_3$  polymorphs at the intermediate stage, prior to mullite formation during heating process. These results confirmed the formation of Al–Si spinel phase instead of  $\gamma$ - $\text{Al}_2\text{O}_3$ . Besides Al–Si spinel formation, it also indicated that the so-called  $\theta$ - $\text{Al}_2\text{O}_3$ , which formed in the intermediate stage, also contains  $\text{SiO}_2$  and it decomposed to mullite and  $\alpha$ - $\text{Al}_2\text{O}_3$  on further heating instead of crystallization of both forms of  $\theta$ - $\text{Al}_2\text{O}_3$  and  $\alpha$ - $\text{Al}_2\text{O}_3$ .

Concerning the growth process of Al–Si spinel phase, Table 3 indicates that the XRD intensity ratio of Al–Si spinel phase to amorphous band increases in the entire range of temperature from 600 to 1200 °C for DG40 and DG66 and from 600 °C up to 1100 °C for DG72. In the temperature range between 900 and 1000 °C, following two phenomena occur simultaneously. When the intensity of X-ray amorphous band decreases (Fig. 4), the crystallization of accumulated aluminosilicate (A) phase leading to the formation of Al–Si spinel phase starts (Fig. 6). Therefore, these two events are interrelated. It is interpreted that crystallization of Al–Si spinel occurs beyond 950 °C from aluminosilicate (A) phase itself.

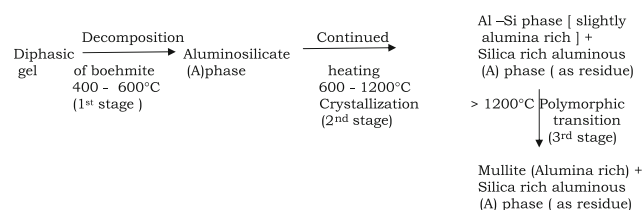


The existence of XRD band at  $22^\circ 2\theta$  during heat treatment of diphasic gels beyond  $1000^\circ\text{C}$  confirms the presence of remaining silica-rich aluminous (A) phase. Table 3 shows that ratio of intensity of Al–Si spinel to amorphous band decreases beyond  $1100^\circ\text{C}$  in case of DG72. This supports amorphous phase development.

Therefore, diphasic gel, in general, may be conceived as a micro composite which during heating in the temperature range of  $600\text{--}900^\circ\text{C}$  develops aluminosilicate (A) phase and some quantity of Al–Si spinel phase and silica-incorporated  $\theta\text{-Al}_2\text{O}_3$  phase. At  $\sim 1000^\circ\text{C}$ , the remaining aluminosilicate (A) phase fully crystallizes to Al–Si spinel phase. A residual amorphous band due to silica-rich aluminous (A) phase remains in association with these phases.

### Polymorphic transformation of Al–Si spinel

As discussed above diphasic gel namely DG40, DG66, and DG72 at  $\sim 1200^\circ\text{C}$  consists of Al–Si spinel phase (major), silica-incorporated  $\theta\text{-Al}_2\text{O}_3$  (minor), and silica-rich alumina (A) phase. The amount of phases varies with the composition of diphasic gel chosen. At the 3rd stage ( $>1200^\circ\text{C}$ ) mullitization commences. It is explained that Al–Si spinel (slightly rich in alumina) formed out of these three diphasic gels polymorphically transforms to mullite (slightly rich in alumina) during heat treatment at  $>1250^\circ\text{C}$  (Figs. 1a, b, and 2a). This mullite transforms to regular 3:2 mullite by solid-state reaction of alumina-rich mullite with silica-rich aluminous (A) phase on further heating. Schematic diagram of phase development of DG40 and DG72 were shown earlier [13]. The probable sequence of transformation of diphasic gel which was presented vide Eq. 1 [13] is now substantiated by incorporation of a new stage as substantiated in the present study. In this stage, an aluminosilicate (A) phase exists as an additional intermediate phase prior to Al–Si spinel formation and it is shown below.



### Mechanism of transformation of alumina phase

#### First mechanism

During heating of diphasic  $\text{Al}_2\text{O}_3\text{-SiO}_2$  gel, it is shown that interaction takes place during dehydroxylation among two reactants and develops aluminosilicate glassy phase. This is

more predominant in diphasic gels with decrease in wt.% of  $\text{Al}_2\text{O}_3$  composition from DG72 to DG66 to DG40, as a consequence XRD peak area of amorphous band at  $22^\circ 2\theta$  increases (Fig. 4). This glassy phase seems to retard further transformation of the alumina component or suppress  $\theta\text{-}$  to  $\alpha\text{-Al}_2\text{O}_3$  conversion.

#### Second mechanism

In the transformation of pure  $\theta\text{-}$  to  $\alpha\text{-Al}_2\text{O}_3$ , two steps may occur in the nucleation process as suggested by Bye and Simpkin [24], Xue and Chem [25], and Clark and White [26].

- i. Change in mobility of  $\text{O}^{2-}$  ion arrangement, i.e., close-packed cubic system (CCP) to hexagonal close-packed system (HCP).
- ii. Migration of aluminum cation from tetrahedral to octahedral interstices.

Inhibition in nucleation of  $\alpha\text{-Al}_2\text{O}_3$  may be due to the possibility of formation of solid solution of silicon in  $\gamma\text{-Al}_2\text{O}_3$  since tetrahedral substitution of Si by replacing Al is a feasible proposition. Once Si enters into the lattice, migration of  $\text{Al}^{+3}$  within the alumina grain is not likely initiated as necessary for polymorphic phase change to  $\alpha\text{-Al}_2\text{O}_3$ . Thus, both, two, the mechanisms are operative in the present case of evolution of diphasic gels. Al–Si spinel and/or silicon-incorporated  $\delta\text{-}$  or  $\theta\text{-Al}_2\text{O}_3$  are formed during the heating process of diphasic gel and subsequent structural transformations of these phases are the cause of mullite formation.

#### Discussion of earlier studies

Now we shall discuss the previous literatures on (i) characterization of amorphous band, (ii) other way of the crystallization process of Al–Si spinel phase, and (iii) the composition of it.

#### Characterization of amorphous band

The present study shows that amorphous band which exists in the transformation process of diphasic gels is not free amorphous silica as assumed by various earlier researchers [10, 27–31]. Okada and Otsuka [2] earlier revealed that the chemical composition of the amorphous phase coexisting with the spinel phase was also not merely pure silica, but it contained alumina and it might be corresponded to  $6\text{SiO}_2\cdot\text{Al}_2\text{O}_3$  tentatively. By  $^{29}\text{Si}$  MAS NMR studies, Jaymes et al. [30] and Schneider et al. [15] noted the appearance of a new peak at  $\sim -110$  ppm during the transformation of HB13 and diphasic gel marked B heat treated to  $1000^\circ\text{C}$ . They characterized this  $-110\text{-ppm}$  Si NMR peak as amorphous silica without presenting any

experimental evidence in its favor. According to Engelhardt and Michel [32], in aluminosilicate, the silica tetrahedra with four bridging oxygen atoms are also classified into five species based on the number of adjacent aluminum atoms bonded to oxygen.

Q4(mAl), i.e. Si(OSi) <sub>4</sub> –m(OAl) <sub>m</sub>	Range of chemical shift (ppm)
Q4(4Al)	–81 to –91
Q4(3Al)	–85 to –94
Q4(2Al)	–91 to –100
Q4(1Al)	–97 to –107
Q4(0Al)	–101 to –116

The experimental alkali leaching data (Fig. 6) given in the present study shows the absence of free silica (A). Therefore, the –110-ppm peak is characterized as silica-rich aluminous (A) phase in view of <sup>29</sup>Si MAS NMR data which is near to Q4(1Al) region. The present author [22] showed <sup>29</sup>Si spectrum of different gels heated to 1000 °C. It was shown that as the silica content of the gel decreases, the –110-ppm peak also decreases simultaneously. That result indicated that the content of silica-rich alumina (A) phase formed on heating high alumina-content gel decreased with decreasing concentration of silica content.

#### Characterization of spinel phase

By transmission electron microscopy Schneider et al. [10] noted the occurrence of large spherical particles ( $\leq 0.5 \mu\text{m}$ ) of silica phase and fine-grained aggregates of pseudo-boehmite particles ( $\sim 20 \text{ nm}$ ) in their Type II gel. They showed the decay of those spherical particles during heating process. They conjectured the theory of incorporation of silicon into the agglomerates of  $\gamma$ -alumina and suggested that diffusion process of Si at the surfaces of the  $\gamma$ -alumina crystallites was related to temperature of heating. But it was not known from which phase Si diffuse out. Was it from free silica or from aluminosilicate (A) phase? Present study shows that free silica is not available for diffusion reaction as assumed. Ivankovic et al. [14] suggested the formation process of Al–Si spinel phase as follows.

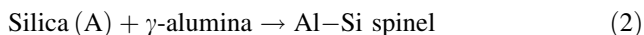


Figure 6 of the present alkali leaching study indicates that free silica (A) does not exist on heating DG72 at  $\sim 800 \text{ }^\circ\text{C}$  as they conceived. This fact is almost true in the entire temperature range from 600 °C (the lowest temperature chosen in the present experiment) up to 1200 °C. Accordingly, the above reaction (2) shown by them does not occur in reality due to unavailability of free silica (A) to react with  $\gamma$ -alumina phase. Therefore, the concept of

Al–Si spinel formation suggested by them [14] seems unacceptable. In the temperature range of 600–900 °C, our X-ray intensity measurement values of band as shown in Fig. 4 show that band due to aluminosilicate (A) phase formation slowly increases.

Apparent relation between the decrease in amorphous band with formation of Al–Si spinel shown by Ivankovic et al. [14] needs explanation. They did not present any mechanism by which Al–Si spinel develops. Present study shows that during dehydroxylation diphasic gel itself decomposes and forms aluminosilicate (A) phase. At the next step, later phase crystallizes to Al–Si spinel in the temperature range of 900–1000 °C and as a result the band intensity decreases. XRD band intensity again increases slightly with further heating to 1200 °C owing to non-crystalline aluminosilicate formation as shown in Fig. 4. Thus, the amorphous band still exists in association with Al–Si spinel and with some unconverted  $\gamma$ -Al<sub>2</sub>O<sub>3</sub> or  $\theta$ -Al<sub>2</sub>O<sub>3</sub> at high temperature. Even in the case of monophasic gel, the present author earlier [13] showed the formation of aluminosilicate (A) phase as an intermediary phase prior to crystallization of either *t*-mullite or a mixture of *t*-mullite and Al–Si spinel phase or solely Al–Si spinel phase. Therefore, the decrease in intensity of amorphous band as observed in the case of Ivankovic et al. [14] for their gel sample marked B is correlated to crystallization of aluminosilicate (A) phase itself to Al–Si spinel phase transformation as shown in the present study and not due to solid-state reaction between silica (A) with  $\gamma$ -alumina as per Eq. (2).

Moreover, they did not succeed to detect the changes in integrated area of spinel peak at  $46^\circ 2\theta$  and same for amorphous band (assuming silica peak) at  $22^\circ 2\theta$  for other two heat-treated diphasic gels marked C and D synthesized from  $\gamma$ -Al<sub>2</sub>O<sub>3</sub>, Degusa and ( $\gamma$ -AlOOH) Boehmite of Disperal varieties, respectively. These might be due to manual selection of background prior to calculating peak intensities. It is thus required to re-examine the applicability of this concept in context to the present study for characterizing spinel phase formed out of different source materials under varying processing techniques. On careful observation of their Fig. 5a and b qualitatively, it is apparent that (i) both the intensity peak due to spinel phase 0.197 nm ( $46^\circ 2\theta \text{ CuK}_\alpha$ ) and 0.139 nm ( $67^\circ 2\theta \text{ CuK}_\alpha$ ) increased with heat treatment from 600 to 1000 to 1200 °C as in the present study, (ii) intensity of amorphous band at  $22^\circ 2\theta \text{ CuK}_\alpha$  decreased from 600 to 1000 to 1200 °C for heat-treated sample marked D. On the contrary, they mentioned that the amount of amorphous silica was almost constant in this temperature range and intensity of  $\gamma$ -Al<sub>2</sub>O<sub>3</sub> increased with temperature. These are obviously due to their unsystematic background selection and calculation of peak area thereof. With use of CaF<sub>2</sub> as calibrant prior to the measurement of

XRD intensities of band and spinel phases, present study shows that the ratios of the intensity peak of spinel phase to that of amorphous band of gel samples of different compositions increase with heat treatment temperature from 900 to 1200 °C (Table 3). Thus, decrease in intensity of amorphous band with increase of the peak of spinel phase further confirms the ongoing crystallization process of aluminosilicate (A) phase itself to form Al–Si spinel phase. Therefore, the present study supports the concept of formation of Al–Si spinel phase as analyzed above.

#### Composition of nano-crystalline spinel phase

Schneider et al. [10] by their EDX analysis showed that silica content of the spinel phase was 12 mol% at 500 °C and increased up to 18 mol% (11.5 wt.% at 1150 °C. This data agree with 8–18 wt.% silica as shown by Okada and Otsuka [2] and later with 10 wt.% silica by Sonuparlak et al. [33], and ~7 wt.% silica by Gerardin et al. [34]. However, this value does not fit well with present author's data [3, 4, 6, 11–13] and others [5, 7, 35]. Recently, the present author critically examined the range of solid solutions of silica in spinel structure [22]. It was shown by XRD that an amount of 24–30 wt.% silica could be accommodated in silica- $\gamma$ -alumina solid solution. Although, we differ in projecting the composition of Al–Si spinel phase, we all agree to the point that Al–Si spinel phase is formed as an intermediate during heating both diphasic gel and in some cases monophasic gel.

#### Conclusions

Diphasic Al<sub>2</sub>O<sub>3</sub>–SiO<sub>2</sub> gels of three different compositions have been synthesized, heat treated, phases formed are identified, and characterized by XRD and by alkali leaching studies. The following conclusions are obtained.

1. At the first stage (400–500 °C), diphasic gel dehydrates during heating and develops aluminosilicate (A) phase.
2. At the second stage (500–900 °C), during continued heating, both the formation of later phase and absence of free silica (A) is confirmed, as evident by alkali leaching study.
3. At the third stage (~1000 °C), the major increase in XRD intensity of spinel phase occurs due to sudden decrease in intensity of amorphous band of aluminosilicate(A) phase. It remains stable up to as high as 1200 °C during phase evolution process. The precise XRD chart and pattern of the intermediate spinel phase are different from those of pure  $\gamma$ - or  $\delta$ - or  $\theta$ -Al<sub>2</sub>O<sub>3</sub> and it is identified as Al–Si spinel phase with (slightly rich in alumina).

4. At the fourth stage (beyond 1200 °C), Al–Si spinel phase rapidly transforms to mullite (alumina-rich) during heating >1250 °C.

The mechanism of transformation of alumina component of diphasic gel in the presence of silica is discussed.

**Acknowledgement** The author thanks the Director, Dr. H.S. Maity for his kind permission to publish this paper and also thanks Mr. P. Nandy for the graphic and art work.

#### References

1. Schmuecker M, Schneider H (2005) In: Schneider H, Komarneni S (eds) Mullite. Wiley-VCH, Weinheim, Germany, pp 167–189
2. Okada K, Otsuka N (1986) J Am Ceram Soc 69:652
3. Chakraborty AK (1978) J Am Ceram Soc 61:170
4. Chakraborty AK (1979) J Am Ceram Soc 62:120
5. Low M, McPherson R (1989) J Mater Sci 24:926
6. Chakraborty AK, Ghosh DK (1986) J Am Ceram Soc 69:C-202
7. Suzuki H, Saito H, Tomokiyo Y, Suyama Y (1990) In: Somya S, Davas RF, Pask JA (eds) Ceramic transactions, vol 8. American Ceramic Society, Westerville, OH, p 263
8. Chakraborty AK, Ghosh DK (1987) J Am Ceram Soc 70:C46
9. Chakraborty AK (1993) J Mater Sci 28:3839
10. Schneider H, Voll D, Saruhan B, Schmucker M (1994) J Eur Ceram Soc 13:441
11. Chakraborty AK, Das S (2003) Ceram Int 29:27
12. Chakraborty AK (2004) Br Ceram Trans 103:33
13. Chakraborty AK (2005) J Am Ceram Soc 88:134
14. Ivankovic H, Tkalec E, Nass R, Schmidt H (2003) J Eur Ceram Soc 23:283
15. Schneider H, Saruhan B, Voll D, Merwin L, Sebald A (1993) J Eur Ceram Soc 11:87
16. Chakraborty AK (1996) J Therm Anal 46:1413
17. Iller RK (1964) J Am Ceram Soc 47:339
18. Yoldas BE (1976) J Mater Sci 11:465
19. Yoldas BE (1980) Am Ceram Soc Bull 59:479
20. Wakao Y, Hibino T (1962) Nagoya Kogyo Gijutsu Shikensho Hokoku 11:588
21. Saito Y, Takei T, Hayashi S, Yasumori A, Okada K (1998) J Am Ceram Soc 81:2197
22. Chakraborty AK (2006) Adv Appl Ceram 105:297
23. Chakraborty AK (submitted) Heating effects of mixed (boehmite–TEOS) and impregnated ( $\gamma$ -Al<sub>2</sub>O<sub>3</sub>-TEOS) gels. JSST
24. Bye G, Simpkin GT (1974) J Am Ceram Soc 57:367
25. Xue LA, Chem IW (1992) J Mater Sci Lett 11:443
26. Clark PW, White J (1950) Trans Br Ceram Soc 49:305
27. Wei WC, Halloran JW (1988) J Am Ceram Soc 71:166
28. Li DX, Thomson WJ (1991) J Am Ceram Soc 74:574
29. Sundarsan S, Aksay IA (1991) J Am Ceram Soc 74:2388
30. Jaymes I, Douy A, Massiot D, Coutures JP (1996) J Mater Sci 31:4581
31. Ruscher CH, Schrader G, Gotte M (1996) J Eur Ceram Soc 16:169
32. Engelhardt G, Michel D (1987) High resolution solid state NMR of silicates and zeolites. Wiley, New York
33. Sonuparlak B, Sarikaya M, Aksay IA (1987) J Am Ceram Soc 70:837
34. Gerardin C, Sundaresan S, Benziger J, Navrotsky A (1994) Chem Mater 6:160
35. Srikrishna K, Thomas G, Martinez R, Corral MP (1990) J Mater Sci 25:607